

Laser Conditioning Characterization and Damage Threshold Prediction of Hafnia/Silica Multilayer Mirrors by Photothermal Microscopy

A. B. Papandrew, C. J. Stolz, Z. L. Wu, G. E. Loomis, and S. Falabella

This article was submitted to XXXII Annual Symposium on Optical Materials for High Power Lasers, October 16-18, 2000, Boulder, Colorado

U.S. Department of Energy

Lawrence
Livermore
National
Laboratory

December 11, 2000

This document was prepared as an account of work sponsored by an agency of the United States Government. Neither the United States Government nor the University of California nor any of their employees, makes any warranty, express or implied, or assumes any legal liability or responsibility for the accuracy, completeness, or usefulness of any information, apparatus, product, or process disclosed, or represents that its use would not infringe privately owned rights. Reference herein to any specific commercial product, process, or service by trade name, trademark, manufacturer, or otherwise, does not necessarily constitute or imply its endorsement, recommendation, or favoring by the United States Government or the University of California. The views and opinions of authors expressed herein do not necessarily state or reflect those of the United States Government or the University of California, and shall not be used for advertising or product endorsement purposes.

This work was performed under the auspices of the U.S. Department of Energy by University of California, Lawrence Livermore National Laboratory under Contract W-7405-Eng-48.

Laser conditioning characterization and damage threshold prediction of hafnia/silica multilayer mirrors by photothermal microscopy

A. B. Papandrew^b, C. J. Stolz^{*a}, Z. L. Wu^c, G. E. Loomis^a, and S. Falabella^a

^aUniversity of California, Lawrence Livermore National Laboratory
P. O. Box 808, L-487, Livermore, CA 94550

^bCurrent affiliation: Division of Engineering and Applied Science
California Institute of Technology, Pasadena, CA 91125

^cCurrent affiliation: Oplink Communications Inc, San Jose, CA 95134

ABSTRACT

Laser conditioning has been shown to improve the laser damage threshold of some optical coatings by greater than 2×. Debate continues within the damage community regarding laser-conditioning mechanisms, but it is clear that nodular ejection is one of the byproducts of the laser conditioning process. To better understand why laser conditioning is so effective, photothermal microscopy was used to measure absorption of coating defects before and after laser exposure. Although a modest absorption reduction was expected due to the lower electric field peaks within a pit and the absence of potentially absorbing nodular seeds, surprisingly, absorption reductions up to 150× were observed.

Photothermal microscopy has also been successfully used to correlate laser-induced damage threshold and absorption of defects in hafnia/silica multilayer optical coatings. Defects with high absorption, as indicated by high photothermal signal, have low damage thresholds. Previously a linear correlation of damage threshold and defect photothermal signal was established with films designed and damage tested at 1ω (1053 nm) and Brewster's angle (56.4°), but characterized by photothermal microscopy at 514.5 nm and near-normal angle of incidence (10°). In this study coatings designed, characterized by photothermal microscopy, and damage tested at the same wavelength, incident angle, and polarization did not have a correlation between defect photothermal signal and absorption.

1. INTRODUCTION

Hafnia/silica multilayer transport mirrors are the 1ω (1053 nm) fluence-limiting components on the National Ignition Facility (NIF), a 1.8-MJ, 192-beam, frequency-tripled laser capable of fusion ignition.¹⁻² These transport mirrors must operate at a minimal fluence of 22 J/cm² at 3 ns pulse length. In order to improve coating lifetimes to minimize laser operating costs, laser damage threshold and growth studies at Lawrence Livermore National Laboratory (LLNL) have been focussed on defect characterization techniques and laser interaction experiments.

Traditionally, laser damage threshold studies have involved post-mortem investigation of damaged defect sites. Unfortunately, this method requires the investigator to deduce information about the damage initiators from only the damage morphology because the damage initiator is annihilated during the explosive damage event. Previous attempts to nondestructively identify fluence-limiting defects by various microscopy techniques such as Scanning Electron Microscopy (SEM), Atomic Force Microscopy (AFM), and Optical Microscopy (OM) have only identified critical geometrical features or scatter characteristics of coating defects and laser damage threshold.³⁻⁷ However, these instruments give no insight into seed stoichiometry or absorption.

Photothermal microscopy holds particular promise for nondestructive identification and characterization of fluence-limiting coating defects.⁸⁻⁹ These defects are particularly difficult to find because they are rare events covering less than 2×10⁻⁴ of the surface area of a 0.34 m² optic. A strong correlation was reported between absorption and laser damage threshold as illustrated in figure 1.¹⁰ Therefore, by using this technique, it is possible to identify the highest absorbing defects for further study to infer their origin. Without this information, it is difficult to accurately determine where in the coating process resources should be devoted for damage threshold improvement. Once fluence-limiting coating defects are identified, laser conditioning programs isolated to the defect site may be identified instead of the "one size fits all" approach currently in use.

For example, a one-step laser conditioning routine has proven adequate for Beamlet optics.¹¹ A gentler conditioning routine, however, may yield a higher damage threshold resulting in greater safety margin for the NIF transport mirrors. The traditional R:1 conditioning test used on small samples consists of 300 pulses slowly increasing in fluence.¹² Single-step conditioning of a NIF optic will take about one day. A R:1 conditioning routine over the entire NIF optic would take approximately 300 days. Full aperture R:1 conditioning is obviously impractical; however, isolation of critical fluence-

* Correspondence: Email: stolz1@llnl.gov; Telephone: 925-422-3562; Fax: 925-422-1210

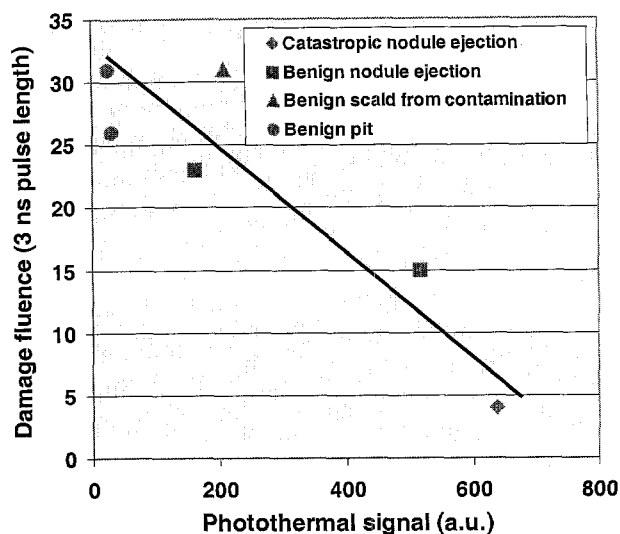


Fig. 1 1ω fluence-limiting defect has highest 2ω photothermal signal.

threshold coatings at 1ω . In order to achieve adequate film stoichiometry, a RF plasma was used to assist in improving film stoichiometry. The setup of this Plasma Assisted Deposition (PAD) process is similar to the Ion Assisted Deposition (IAD) process except a plasma source is used instead of an ion gun. A schematic of the PAD process is in Fig. 2.

Stoichiometry of the SiO_2 layers were evaluated by measuring the UV transmission of a single layer deposited on a fused silica witness. A Cary 5 spectrophotometer was used to measure the transmission of the films. Examination of the transmission spectra in Fig. 3 clearly shows two conclusions. Evaporation of silicon in a reactive environment without plasma assistance results in substoichiometric SiO_x films as illustrated by the higher UV absorption edge compared to a standard silica film evaporated from silica. With plasma assist from oxygen flowing through a 100 Watt, Rf hollow-cathode

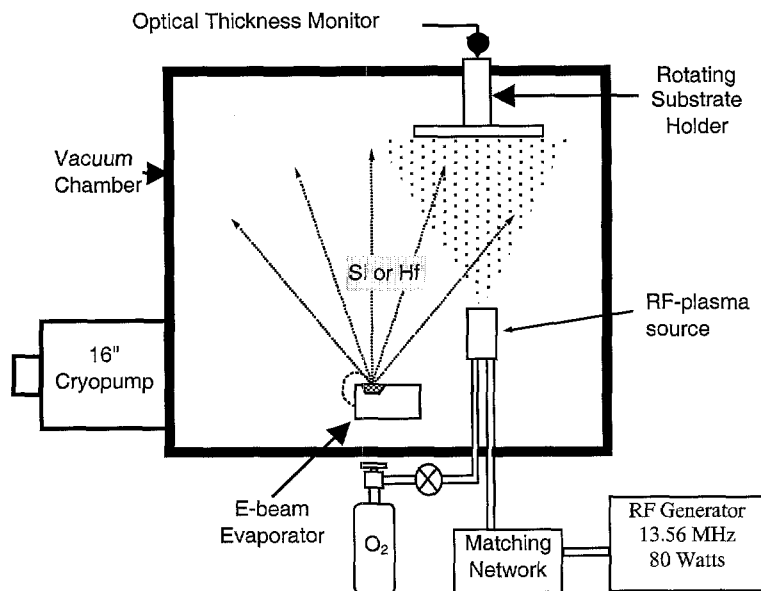


Fig. 2. Schematic of Plasma-Assisted Deposition (PAD) process used to manufacture HfO_2 and SiO_2 multilayers from Hf and Si starting materials.

discharge, the film has an absorption edge similar to the fused silica witness and a refractive index closer to bulk as indicated by the lower amplitude oscillations compared to the film evaporated from silica. This result implies a lower porosity film as would be expected from a higher energetic deposition process, although humidity-induced spectral shifts have not yet been done to confirm film porosity.

2. DEPOSITION PROCESS

Previous work has demonstrated improved quality films for high damage threshold applications can be generated by Physical Vapor Deposition (PVD) from hafnium in a metallic form and silica in an oxide form using an electron beam in a reactive environment.¹³⁻¹⁴ Coatings deposited from only oxide sources have significantly more defects, lower deposition plume stability, and greater interface voids. Based on these results, a PVD process was developed to grow oxide films starting from only metallic sources. One of the traditional problems with silicon evaporation by e-beam is the difficulty growing stoichiometric silica layers. High damage threshold films require low absorption at the operating wavelength. Therefore, Si, SiO , or SiO_x films are unacceptable materials for high damage

threshold coatings at 1ω . One point of concern with higher-energy deposition processes is the severity of the adherence of coating defects within the multilayer. Processes such as IAD and Ion Beam Sputtering (IBS) have defects that are tightly bounded to the multilayer. Although sufficiently large defects that eject at NIF fluences are rare, their ejection is catastrophic.¹⁵ This results in unstable damage sites that grow with repeated irradiation as illustrated in Fig. 4. Therefore, a minimum plasma density was selected that would result in films with adequate stoichiometry, yet minimal mobility of the arriving molecules for loosely bound defects.

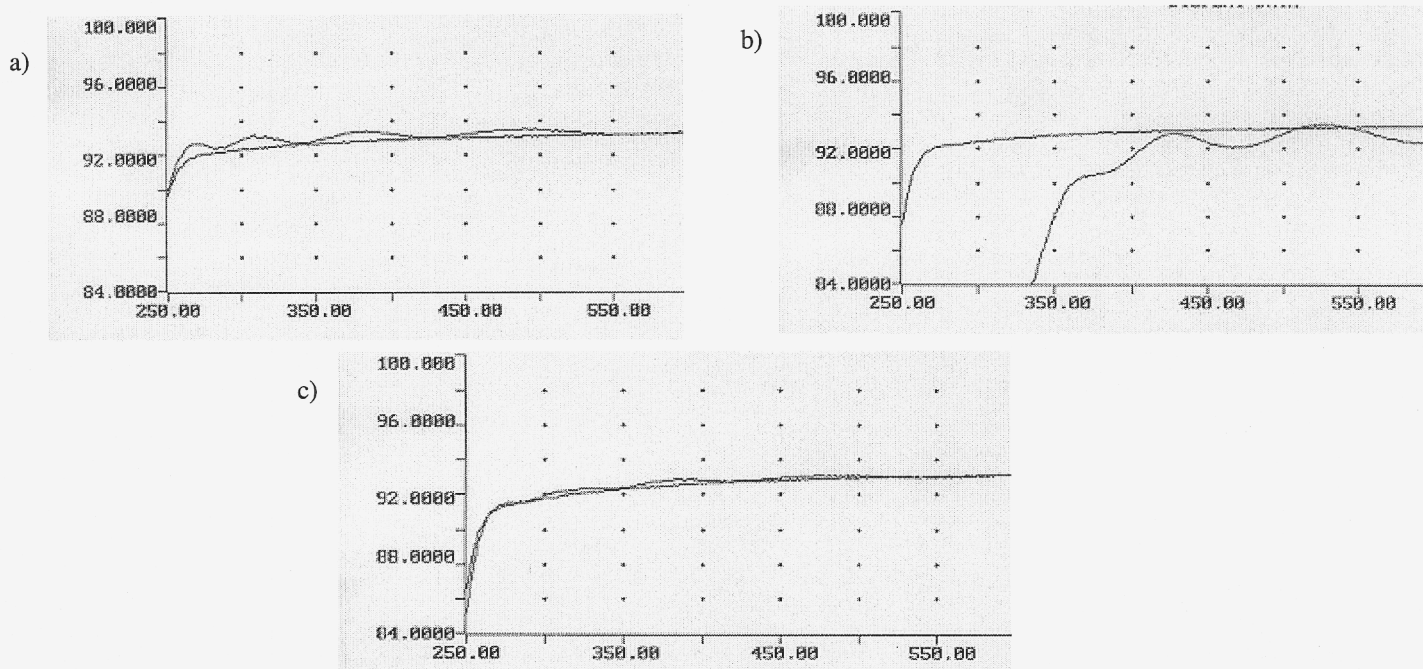


Fig. 3 UV spectra of films grown on silica substrates under the following conditions; a) SiO_2+O_2 with no RF plasma, b) $\text{Si}+\text{O}_2$ with no RF plasma, and c) $\text{Si}+\text{O}_2$ with RF plasma.

3. EXPERIMENTAL APPARATUS

The photothermal microscope used in this work is based on the Surface Thermal Lens (STL) effect described elsewhere.¹⁶⁻¹⁷ In summary, a chopped focussed pump beam is the time-varying heat source. Thermal-induced coating surface modifications due to the interaction of the pump beam and coating defects diffracts a separate larger probe beam. A detector with a lock-in amplifier collects the signal that isolates the time-varying thermal-induced surface morphological changes. The sample is scanned past the coaligned pump and probe beams with an automated scanning system to generate reproducible photothermal images. The 3- μm pump beam limits the spatial resolution of this instrument. One significant drawback of this microscope is the time required to perform a scan. At 3- μm resolution, a 50 $\mu\text{m} \times 50 \mu\text{m}$ scan takes approximately 1 hour. Therefore, without development to improve the data acquisition rate and scanning areas, this instrument is only useful for experiments on very small coating areas.

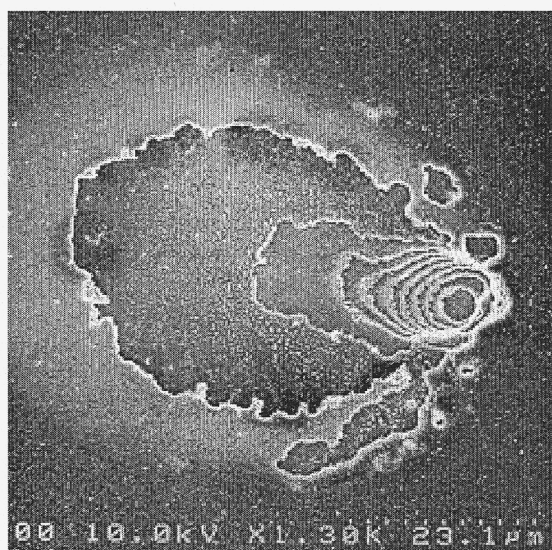


Fig. 4 SEM image of catastrophic damage created by nodular ejection from an IBS coating.

Details of the damage testing system, termed Chameleon, are published elsewhere.¹² A brief description of the damage testing system is given as follows. The damage laser beam (TEM_{00} mode; 532 nm in wavelength, and 3 ns in pulse width) from a Coherent Infinity laser was incident on the sample surface at the design angle of the coating. The beam has a Gaussian shape profile with a diameter around 1.0 mm at $1/e^2$ measured at normal incidence at the sample plane. The sample was monitored in real time using both an OM with a CCD camera and a 0.633 μm He-Ne scattering diagnostic system for damage detection. Laser damage was observed with an OM. An AFM was used to validate nodular ejection.

4. EXPERIMENT

The coatings were deposited on super polished BK7 substrates at LLNL in the Vacuum Process Laboratory (VPL). The coating chamber is a modified Balzer 600 series 3' \times 3' \times 3' box pumped by a CTI 16" CYRO-Torr 400. Hafnia/silica multilayer mirrors were prepared by the PAD process with hafnium and silicon starting materials. The design consisted of 20 alternating layers, including a silica halfwave overcoat as indicated by the following design; sub:(HL)¹⁰ L:air. for a total physical thickness of 1.7 μm . The design wavelength is 532 nm and

incidence angle is 10 degrees. The deposition temperature started at 170°C and finished at 185°C. The oxygen backfill was 9×10^{-5} Torr and deposition rates were 2 Å/sec for both silicon and hafnium. The deposition angle ranged from 30-40 degrees with the substrates in a single axis rotation platen to allow for complete and continuous plasma assisted deposition. The RF plasma source was mounted 12" from the platen. The plasma density previously determined by the silica stoichiometric studies was used.

The mirrors were visually characterized with an OM to identify potentially interesting coating defects. The position of each defect site was measured on a x-y stage for ease of defect location on the various microscopes and damage tester. The defects were then scanned with an AFM for peak-resolution imaging and classification of defect type such as a pit or nodule. They were then measured for absorption with a PTM. The peak-to-average signal, defined as the highest photothermal signal observed within the defect region divided by the average signal in a "defect free" region of the coating, is illustrated in Fig. 5. The sites were then damage tested or laser conditioned. The definition used for damage was any observable change in the sample viewed at 200× with an OM. For conditioning-induced changes not observed with the OM, an AFM was used to characterize the defect after laser irradiation. Finally the sites were characterized with the PTM to examine the influence of laser conditioning on the photothermal signal.

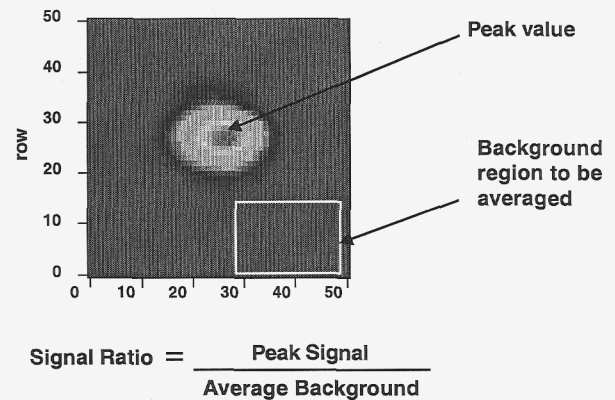


Fig. 5 Illustration of photothermal map of a typical defect and method to calculate peak-to-average signal.

5. RESULTS

Two classes of absorbing defects were identified; nodule and "splash" defects as illustrated in figure 6. Nodules are formed by defect seeds such as spatter caused by the interaction of the electron beam and the starting material, flakes from coating chamber surfaces, or arcing-induced flakes that are incorporated into the film during the deposition process.¹⁸ The splash defects represent a new defect morphology unique to this deposition process. The height of these defects, measured with an AFM, were extremely shallow, typically 50 nm. The peak height measured on a splash defect is 200 nm. This is an order of magnitude smaller than that observed for the nodules in this study which were as tall as 2.3 μm. The lateral dimension however is quite extensive, on the 100 μm scale, therefore, these defects have a "pancake-like" structure. There was a significant amount of spatter observed during the silicon evaporation. This combined with a high deposition angle of 30-40 degrees suggests molten spatter that skips or splashes across the surface as the likely defect origin.

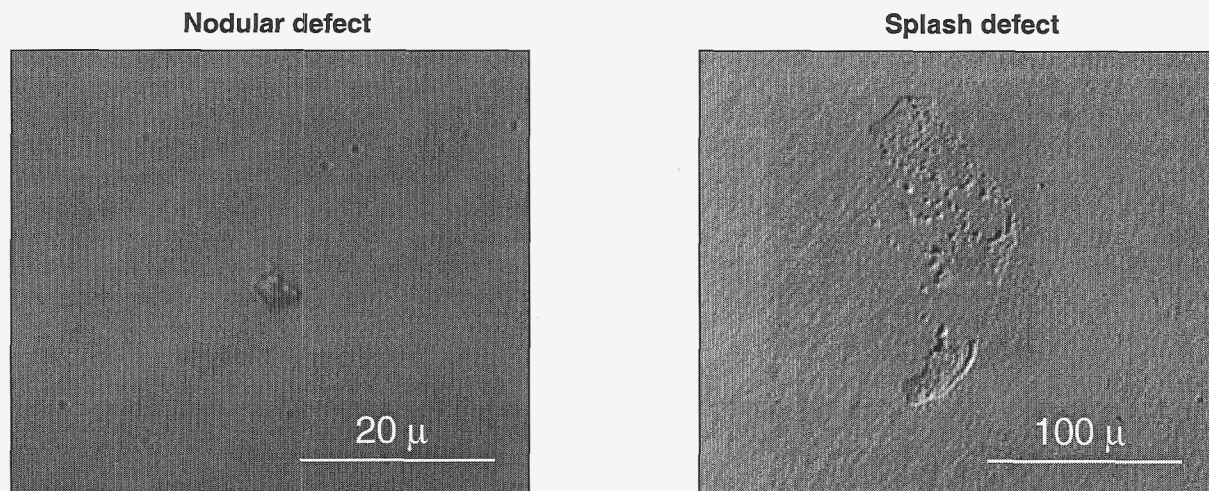


Fig. 6. Optical micrographs of two defect types observed, nodular (left) and splash (right), on hafnia silica films deposited from hafnium and silicon with the PAD process.

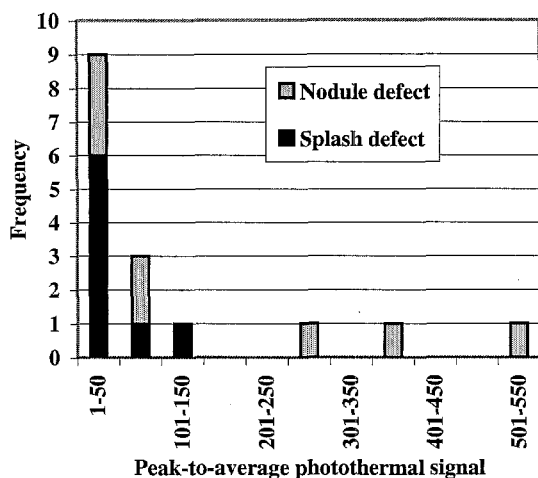


Fig. 7 Histogram of photothermal signal illustrates that splash defects tend to have lower absorption than nodular defects.

electric field distribution and spectral characteristics, particularly for deep defects is negligible. Therefore, deep splash defects will have very little energy absorption when measured with a wavelength within the reflection band of the coating and hence a low photothermal signal. For example, a splash defect on the substrate would have an electric field reduction of approximately 100×. Since the splash defects show little absorption, it is assumed that the splash defects characterized in this study were either deep within the coating stack or were stoichiometric oxides and hence non-absorbing. Nodular defects, however, have a geometrically-enhanced electric field as high as 4× as described elsewhere¹⁹ so a significant photothermal signal is expected for nodular defects, particularly those with large heights such as the 2.3 μm tall nodular defect described above.

5.2. Defect absorption reduction by laser conditioning

Laser conditioning is a process where an optic is irradiated at progressively higher fluences to increase the optics laser damage threshold.²⁰⁻²¹ Nodular ejection has been identified as a mechanism for laser damage threshold improvement by laser conditioning.²²⁻²³ Unfortunately there has been little experimental understanding of why this occurs. Theoretical models suggest a reduction in the geometrically-enhanced electric field profile between a nodule and a nodular ejection pit.¹⁹ Laser-interaction studies reveal that smooth pits from nodular ejections have increased laser damage thresholds.²²⁻²³

Results of this study demonstrate up to 156× reduction in the nodular defect absorption as illustrated in Fig. 8. A nodule defect illustrated in Fig. 9 has quite high absorption compared to the pit created after nodular ejection as shown in Fig. 10. This significant absorption reduction demonstrates the benign nature of nodular ejection pits created by laser conditioning and hence their stability with higher fluence laser exposure.

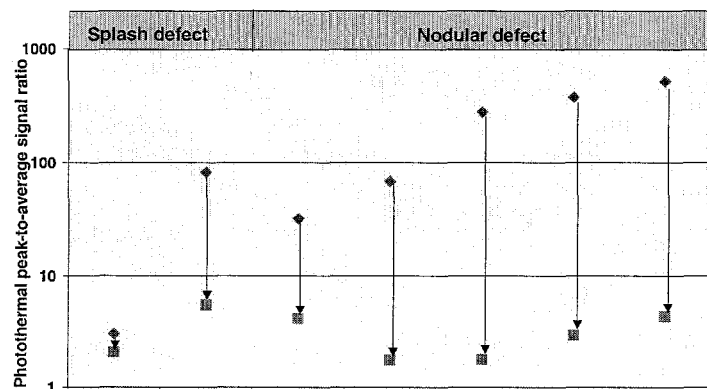


Fig. 8 Peak-to-average signal is reduced 1.5 – 156× for a range of defects after laser conditioning.

5.1. Defect absorption before laser exposure

Photothermal peak-to-average signal of the defects ranged from 1.7 to 516 as illustrated in Fig. 7. This is a 4× enhancement over previously reported 1 ω coatings deposited from a silica and hafnium source compared to these 2 ω films which were deposited from a silicon and hafnium source. A cause of the difference between the two studies might be explained by the low sample size of defects, particularly in the previous study. Another possibility is the stoichiometry of these seeds may be significantly different than in the previous study. Defect cross-section analysis of similar 1 ω coatings deposited from silica reveal a predominance of irregular shaped silica seeds, most likely from solid chunks of silica starting material.¹⁸ The coatings deposited for this study had no oxide starting materials so it is unlikely that “large” defects originating from source material would become fully oxidized.

The absorption of the splash defects tends to be lower than the nodular seeds as illustrated in Fig. 7. These defects can be approximated as a rectangular slab, with typical dimension of 50 μm \times 100 μm \times 0.03 μm . Assuming no edge effects, the impact on the

A smaller absorption reduction of up to 15× was observed with the splash defects. Figure 11 illustrates the absorption of a splash defect. Interestingly there is little correlation with the geometrical features of the splash defect and the photothermal signal. After laser conditioning, the absorption was reduced as illustrated in Fig. 12, however, no detectable morphological change occurred indicating a different laser conditioning mechanism than that associated with defect ejection.

Since the electric field profile does not change, absorption reduction in the defect must be the result of a laser annealing mechanism such as improvement in stoichiometry or reduction of crystalline lattice defects.

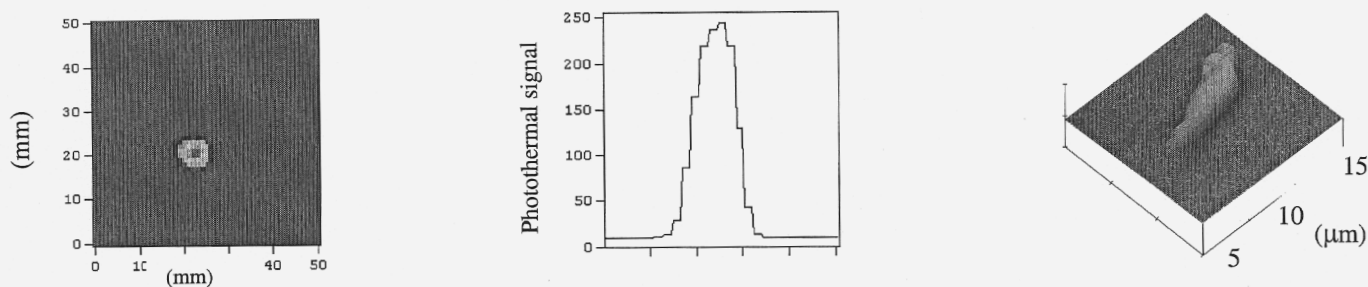


Fig. 9 Photothermal and optical micrograph of a nodule defect before laser exposure.

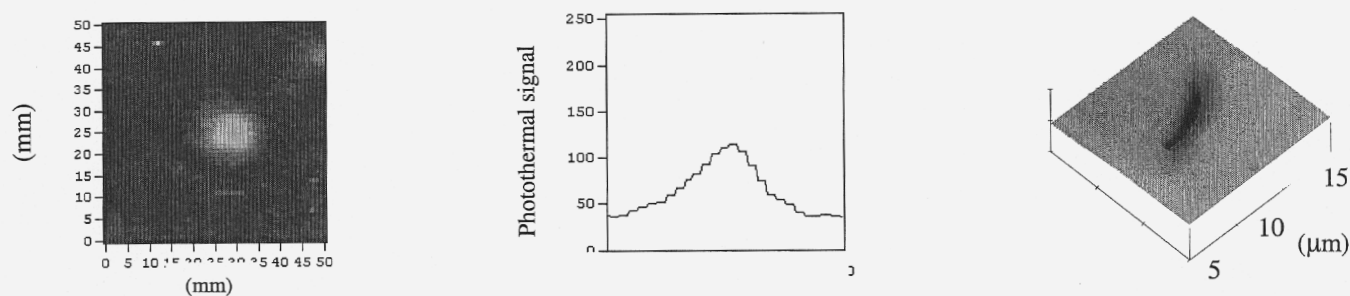


Fig. 10 Photothermal and optical micrograph of a nodule defect after laser conditioning (2 J/cm^2 at 3 ns).

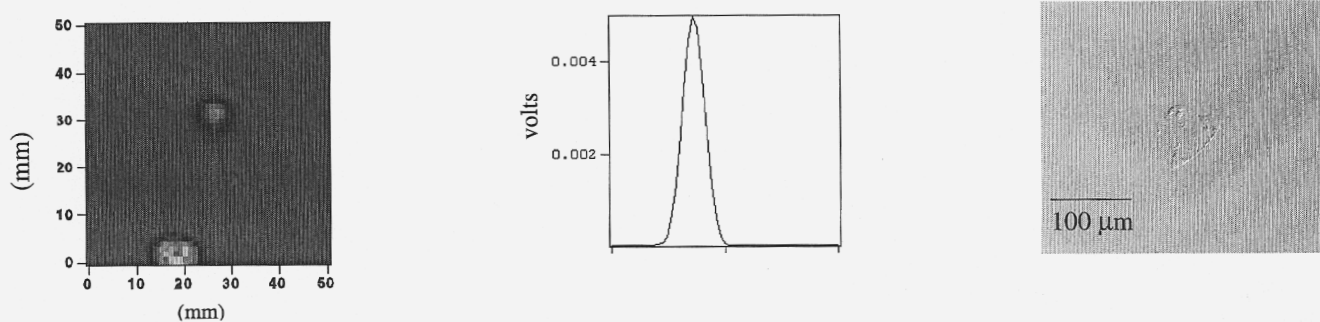


Fig. 11 Photothermal and optical micrograph of a splash defect before laser exposure.

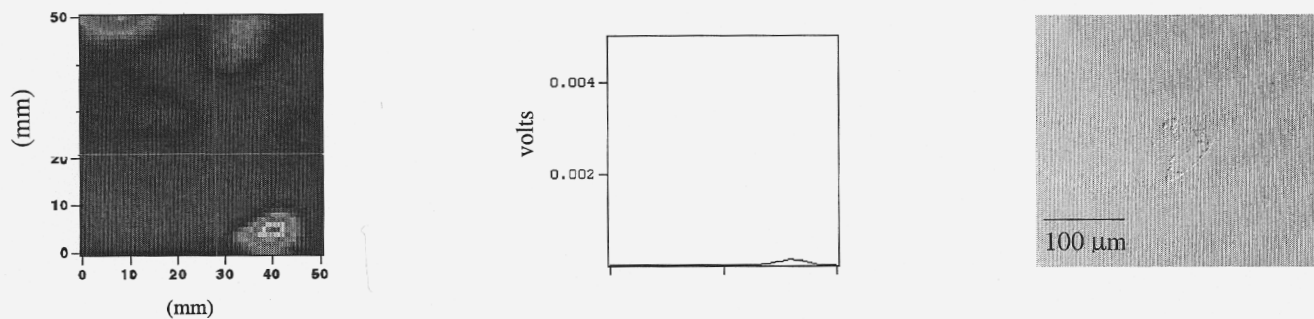


Fig. 12 Photothermal and optical micrograph of a splash defect after laser exposure.

5.3. Correlation of damage threshold and photothermal signal

The damage threshold of the splash defects was essentially the same as the bulk film. Therefore, no correlation exists between peak-to-average photothermal signal and damage threshold. Given the low absorption of the splash defect, particularly after laser conditioning, it is not surprising that these defects do not act very different than the bulk film. Unlike the 1ω coatings in the previous study nodular defects, also did not correlate as illustrated in Fig. 13.

One possible explanation for this discrepancy was a more stringent damage definition. The damage criteria in the previous study was based on measured changes in scattered light while in this study it was based on visual changes at 200 \times optical microscopy. Additionally, the 1 ω coating has a high transmission while the 2 ω coating has a high reflection at the photothermal wavelength. It has been proposed that deep nodular defects are indeed very critical to laser damage at 1 ω .⁷ These deep nodules in a highly transmitting coating will see more energy than deep nodules in a high reflector. The most likely explanation is ejection of deep nodules will likely be more catastrophic in the 1 ω coatings. Typical nodules have voids at the nodule multilayer interface. For deep nodules, these voids begin to "heal" toward the surface of the film. This results in an improved interface between the nodule and multilayer that during ejection may not yield causing fractures along the interfaces of the different coating materials. Fracture along the multilayer interfaces is a significantly more catastrophic than fracture along the nodular boundary. NIF 1 ω HR coatings are typically 2-3 \times thicker than these 2 ω coatings so significantly deeper nodules existed in the previously tested 1 ω coatings.

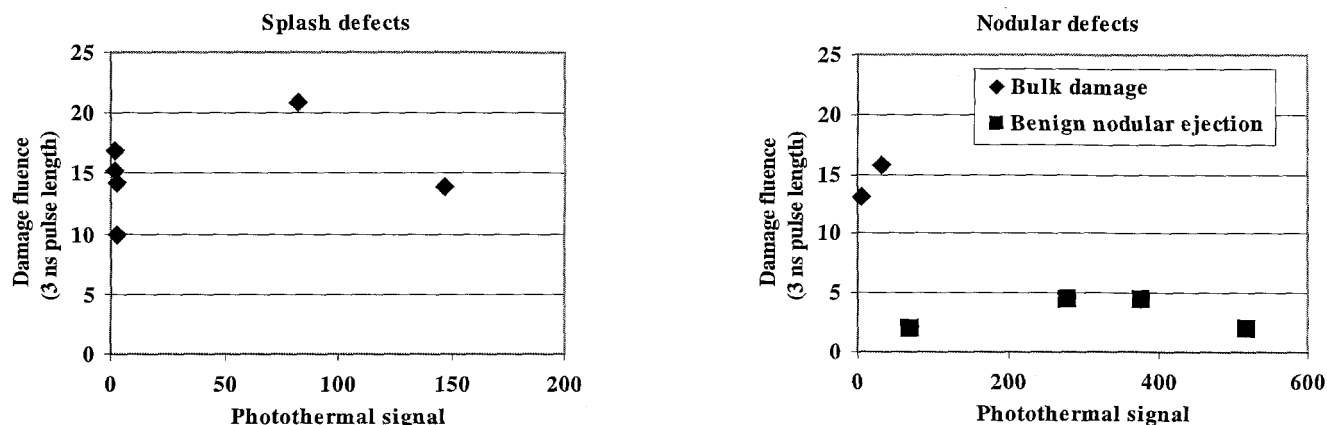


Fig. 13 Poor correlation between photothermal signal and laser damage threshold for splash (left) and nodular (right) defects characterized at 2 ω and damage tested at 2 ω .

6. CONCLUSIONS

Stoichiometric hafnia and silica films can be produced by evaporation of hafnium and silicon in a reactive environment with a plasma assist process. This process has a new class of defects, however the damage threshold of these defects is comparable to the bulk film so are of little consequence. Photothermal microscopic characterization of these coating defects has provided experimental insight into the laser conditioning process, namely the reduction of absorption in the splash defects and nodular ejection pits. Nodular ejection appears to be more benign in 2 ω coatings given the thinner film thickness of 1 ω coatings. Photothermal characterization at wavelengths that are transmissive to the coating may also help identify deep critical defects due to higher energy deposition.

7. ACKNOWLEDGEMENTS

The authors would like to acknowledge the support of Sandra Hadley in preparing this manuscript. The authors would also like to acknowledge the LLNL microscopy support of Jim Hughes (AFM) and Aaron Leanhardt (PTM) who is now a graduate student at MIT. This work was performed under the auspices of the U.S. Department of Energy by Lawrence Livermore National Laboratory under contract No. W-7405-Eng-48.

8. REFERENCES

1. J. A. Paisner, W. H. Lowdermilk, J. D. Boyes, M. S. Sorem, and J. M. Soures "Status of the National Ignition Facility project", *Fusion Engineering and Design* **44**, 23-33 (1999).
2. B. Van Wonterghem, J. R., Murray, J. H. Campbell, D. R. Speck, C. Barker, I. Smith, D. Browning, and W. Behrendt, "Performance of a prototype, large-aperture multipass Nd-glass laser for inertial confinement fusion", *Appl. Opt.* **36**, 4932-4953 (1997).
3. R. J. Tench, R. Chow, and M. R. Kozlowski, "Characterization of defect geometries in multilayer optical coatings", *J. Vac. Sci. Technol. A* **12**, 2808-2813 (1994).
4. M. R. Kozlowski, R. J. Tench, R. Chow, and L. Sheehan, "Influence of defect shape on laser-induced damage in multilayer coatings", in *Optical Interference Coatings*, Florin Abelés, ed., *Proc. Soc. Photo-Opt. Instrum. Eng.* **2253**, 743-750 (1994).

5. M. Poulingue, H. Leplan, J. Dijon, B. Rafin, and M. Ignat, "Generation of defects with diamond and silica particles inside a high reflection coatings: influence on the laser damage threshold", in *Advances in Optical Interference Coatings*, C. Amra and H. A. Macleod, eds., Proc. Soc. Photo-Opt. Instrum. Eng. **3738**, 325-336 (1999).
6. M. Poulingue, J. Dijon, P. Garrec, P. Lyan, "1.06 μm laser irradiation of high reflection coatings inside a scanning electron microscope", in *Laser-Induced Damage in Optical Materials: 1998*, G. J. Exarhos, A. H. Guenther, M. R. Kozlowski, K. L. Lewis, and M. J. Soileau, eds., Proc. Soc. Photo-Opt. Instrum. Eng. **3578**, 188-195 (1999).
7. J. Dijon, M. Poulingue, and J. Hue, "Thermomechanical model of mirror laser damage at 1.06 μm . Part 1: nodule ejection.", in *Laser-Induced Damage in Optical Materials: 1998*, G. J. Exarhos, A. H. Guenther, M. R. Kozlowski, K. L. Lewis, and M. J. Soileau, eds., Proc. Soc. Photo-Opt. Instrum. Eng. **3578**, 387-396 (1999).
8. M. Reichling, A. Bodemann, N. Kaiser, "Defect-induced laser damage in oxide multilayer coatings for 248 nm," *Thin Solid Films* **320**, 264-279 (1998).
9. C. J. Stolz, J. M. Yoshiyama, A. Salleo, Z. L. Wu, J. Green, and R. Krupka, "Characterization of nodular and thermal defects in hafnia/silica multilayer coatings using optical, photothermal, and atomic force microscopy", in *Laser-Induced Damage in Optical Materials: 1998*, G. J. Exarhos, A. H. Guenther, M. R. Kozlowski, K. L. Lewis, and M. J. Soileau, eds., Proc. Soc. Photo-Opt. Instrum. Eng. **3578**, 475-483 (1999).
10. Z. L. Wu, C. J. Stolz, S. C. Weakley, and J. D. Hughes, "Damage threshold prediction of hafnia/silica multilayer coatings by nondestructive evaluation of fluence-limiting defects," *Appl. Opt.*, to be published.
11. C. J. Stolz, L. M. Sheehan, S. M. Maricle, S. Schwartz, and J. Hue, "A study of laser conditioning methods of hafnia silica multilayer mirrors", in *Laser-Induced Damage in Optical Materials: 1998*, G. J. Exarhos, A. H. Guenther, M. R. Kozlowski, K. L. Lewis, and M. J. Soileau, eds., Proc. Soc. Photo-Opt. Instrum. Eng. **3578**, 144-152 (1999).
12. A. J. Morgan, F. Rainer, F. P. DeMarco, R. P. Gonzales, M. R. Kozlowski, and M. C. Staggs, "Expanded damage test facilities at LLNL," in *Laser-Induced Damage in Optical Materials: 1989*, H. E. Bennett, L. L. Chase, A. H. Guenther, B. E. Newnam, and M. J. Soileau, eds., NIST Spec. Publ. **801**, 47-57 (1990).
13. R. Chow, S. Falabella, G. E. Loomis, F. Rainer, C. J. Stolz, and M. R. Kozlowski, "Reactive evaporation of low-defect density hafnia", *Appl. Opt.* **32**, 5567-5574 (1993).
14. C. J. Stolz, L. M. Sheehan, M. K. Von Gunten, R. P. Bevis, and D. J. Smith, "The advantages of evaporation of hafnium in a reactive environment to manufacture high damage threshold multilayer coatings by electron-beam deposition", in *Advances in Optical Interference Coatings*, C. Amra and H. A. Macleod, eds., Proc. Soc. Photo-Opt. Instrum. Eng. **3738**, 318-324 (1999).
15. C. J. Stolz, F. Y. Génin, M. R. Kozlowski, D. Long, R. Lalezari, Z. L. Wu, and P. K. Kuo, "Influence of microstructure on laser damage threshold of IBS coatings," in *Laser-Induced Damage in Optical Materials: 1995*, H. E. Bennett, A. H. Guenther, M. R. Kozlowski, B. E. Newnam, and M. J. Soileau, eds., Proc. Soc. Photo-Opt. Instrum. Eng. **2714**, 351-358 (1996).
16. Z. L. Wu, P. K. Kuo, Y. S. Lu, S. T. Gu, and R. Krupka, "Non-destructive evaluation of thin fin coatings using a laser-induced surface thermal lensing effect," *Thin Solid Films* **291**, 271-277 (1996).
17. R. Chow, J. R. Taylor, Z. L. Wu, Y. Han, and T. Yang, "Absorptance measurements of transmissive optical components by the surface thermal lensing technique", in *Laser-Induced Damage in Optical Materials: 1997*, G. J. Exarhos, A. H. Guenther, M. R. Kozlowski, and M. J. Soileau, eds., Proc. Soc. Photo-Opt. Instrum. Eng. **3244**, 376-385 (1998).
18. C. J. Stolz, R. J. Tench, M. R. Kozlowski, and A. Fornier, "A comparison of nodular defect seed geometries from different deposition techniques", in *Laser-Induced Damage in Optical Materials: 1995*, H. E. Bennett, A. H. Guenther, M. R. Kozlowski, B. E. Newnam, and M. J. Soileau, eds., Proc. Soc. Photo-Opt. Instrum. Eng. **2714**, 374-382 (1996).
19. J. F. DeFord and M. R. Kozlowski, "Modeling of electric-field enhancement at nodular defects in dielectric mirror coatings", in *Laser-Induced Damage in Optical Materials: 1992*, H. E. Bennett, L. L. Chase, A. H. Guenther, B. E. Newnam, and M. J. Soileau, eds., Proc. Soc. Photo-Opt. Instrum. Eng. **1848**, 455-470 (1993).
20. C. R. Wolfe, M. R. Kozlowski, J. H. Campbell, F. Rainer, A. J. Morgan, and R. P. Gonzales, "Lower conditioning of optical thin films," in *Laser-Induced Damage in Optical Materials: 1989*, H. E. Bennett, L. L. Chase, A. H. Guenther, B. E. Newnam, and M. J. Soileau, eds., NIST Spec. Publ. **801**, 360-375 (1990).
21. H. Bercegol, "What is laser conditioning? A review focused on dielectric multilayers", in *Laser-Induced Damage in Optical Materials: 1998*, G. J. Exarhos, A. H. Guenther, M. R. Kozlowski, K. L. Lewis, and M. J. Soileau, eds., Proc. Soc. Photo-Opt. Instrum. Eng. **3578**, 421-425 (1999).
22. M. C. Staggs, M. Balooch, M. R. Kozlowski, and W. J. Seikhaus, "In-situ atomic force microscopy of laser-conditioned and laser-damaged $\text{HfO}_2/\text{SiO}_2$ dielectric mirror coatings", in *Laser-Induced Damage in Optical Materials: 1991*, H. E. Bennett, L. L. Chase, A. H. Guenther, B. E. Newnam, and M. J. Soileau, eds., Proc. Soc. Photo-Opt. Instrum. Eng. **1624**, 375-385 (1992).
23. A. Fornier, C. Cordillot, D. Ausserre, and F. Paris, "Laser conditioning of optical coatings: some issues in the characterization by atomic force microscopy", in *Laser-Induced Damage in Optical Materials: 1993*, H. E. Bennett, L. L. Chase, A. H. Guenther, B. E. Newnam, and M. J. Soileau, eds., Proc. Soc. Photo-Opt. Instrum. Eng. **2114**, 355-365 (1994).